Bioorganic & Medicinal Chemistry Letters 22 (2012) 4404–4409

Contents lists available at SciVerse ScienceDirect

Bioorganic & Medicinal Chemistry Letters

journal homepage: www.elsevier.com/locate/bmcl

Fused tricyclic indoles as $S1P_1$ agonists with robust efficacy in animal models of autoimmune disease

Daniel J. Buzard *, Sangdon Han, Luis Lopez, Andrew Kawasaki †, Jeanne Moody ‡, Lars Thoresen, Brett Ullman, Juerg Lehmann, Imelda Calderon, Xiuwen Zhu, Tawfik Gharbaoui §, Dipanjan Sengupta §, Ashwin Krishnan, Yinghong Gao ¶, Jeff Edwards ‖, Jeremy Barden, Michael Morgan, Khawja Usmani, Chuan Chen, Abu Sadeque, Jayant Thatte ††, Michelle Solomon, Lixia Fu ‡‡, Kevin Whelan, Ling Liu §§, Hussien Al-Shamma, Joel Gatlin, Minh Le, Charles Xing, Sheryll Espinola ¶¶, Robert M. Jones

Arena Pharmaceuticals, 6166 Nancy Ridge Drive, San Diego, CA 92121, USA

ARTICLE INFO

Article history:
Received 29 March 2012
Revised 26 April 2012
Accepted 27 April 2012
Available online 7 May 2012

Keywords:
Sphingosine-1 phosphate receptor
$S1P_1$ agonist
Immunomodulators
FTY720

ABSTRACT

Two series of fused tricyclic indoles were identified as potent and selective $S1P_1$ agonists. In vivo these agonists produced a significant reduction in circulating lymphocytes which translated into robust efficacy in several rodent models of autoimmune disease. Importantly, these agonists were devoid of any activity at the $S1P_3$ receptor in vitro, and correspondingly did not produce $S1P_3$ mediated bradycardia in telemeterized rat.

Fingolimod (**1**) is a potent immunosuppressant that was identified during a medicinal chemistry campaign aimed at dialing out the GI side effect profile associated with the secondary fungal metabolite ISP-1 (**2**, Fig. 1).[1] In vivo, (**1**) is phosphorylated to the (*S*)-isomeric mono-phosphate (**3**) which is an agonist at four of the five sphingosine-1-phosphate receptors ($S1P_1$, $S1P_{3-5}$).[2] The $S1P/S1P_1$ axis regulates the egress of lymphocytes from peripheral lymphoid tissue and (**3**) prevents this trafficking via sustained receptor internalization accompanied by proteasomal degradation.[3] Impaired lymphocyte trafficking reduces the circulation of auto-reactive immune cells, which has been found to slow the progression of disease in multiple sclerosis patients.[4] Fingolimod also may be acting directly on astrocytes to reduce inflammation in the CNS of these patients. $S1P_1$ expression in central MS lesions is dramatically increased, and mouse neural $S1P_1$ knockouts phenotypically show reduced disease severity, astrogliosis, demyelination and axonal loss when compared to their wild type littermates.[5] The precise role of the other S1P subtypes in the amelioration of disease is less well understood, although (**1**) may be acting on the $S1P_5$ and $S1P_3$ receptors expressed centrally on oligodendrocytes and astrocytes.[3]

Over the last decade, medicinal chemistry efforts have focused on identifying alternative agents with improved selectivity. Particular emphasis has been placed on the cardiac expressed $S1P_3$ receptor that is associated with bradycardia in rodents.[6] However, human trials of the $S1P_3$-sparing agonist BAF312, suggests that the transient effect on heart rate may not be attributable to $S1P_3$ activation in humans.[7] More recently, researchers have sought agonists with improved pharmacokinetic profiles given the long half-life of (**1**) in humans ($T_{1/2}$ = 8 days).[8] These efforts have also centered around developing non pro-drug agonists that can penetrate the CNS and act directly on astrocytes.[9] Development of

* Corresponding author.
E-mail address: dbuzard@arenapharm.com (D.J. Buzard).
† Present address: Focus Synthesis, 11475 Sorrento Valley Road, Suite 212, San Diego, CA 92121, USA.
‡ Present address: Regulus Therapeutics, 3545 John Hopkins Court, San Diego, CA 92121, USA.
§ Present address: Dart NeuroScience LLC, 7473 Lusk Boulevard, San Diego, CA 92121, USA.
¶ Present address: EMD Millipore, 10394 Pacific Center Court, San Diego, CA 92121, USA.
‖ Present address: Amylin Pharmaceuticals, 9360 Towne Center Drive, San Diego, CA 92121, USA.
†† Present address: PRESCOS LLC, 3550 General Atomics Court, M/S 02-422, San Diego, CA 92121, USA.
‡‡ Present address: Synthetic Genomics, 11149 North Torrey Pines Road, La Jolla, CA 92037, USA.
§§ Present address: Pfizer, 10646 Science Center Drive, San Diego, CA 92121-1150, USA.
¶¶ Present address: Genomics Institute of the Novartis Research Foundation, 10675 John Jay Hopkins Drive, San Diego, CA 92121, USA.

0960-894X/$ - see front matter © 2012 Elsevier Ltd. All rights reserved.
http://dx.doi.org/10.1016/j.bmcl.2012.04.129

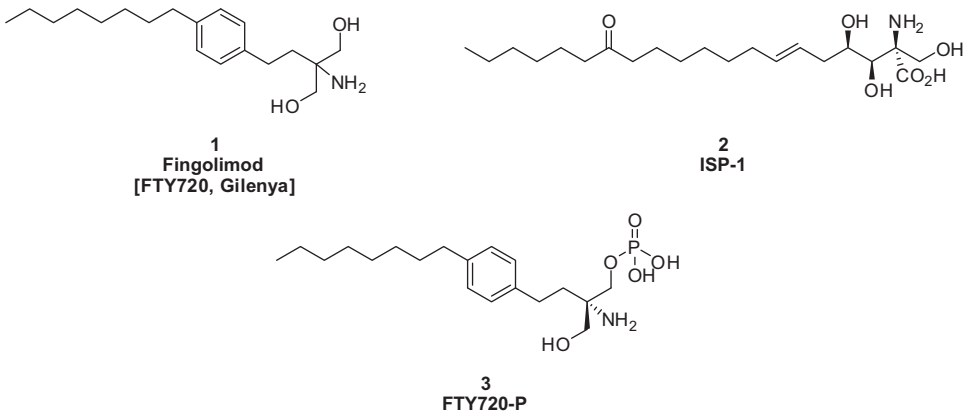

Figure 1. Fingolimod origin and mechanism.

agonists for other autoimmune indications such as psoriasis (Ponesimod),[10] polymyositis (BAF312),[11] and ulcerative colitis (KRP-203)[12] is also underway.

As part of our effort to identify superior $S1P_1$ agonists, we have expanded upon an early series of 3-(indolin-2-yl)propanoic acids (**4**, Fig. 2)[13] and herein disclose two fused tricyclic indole $S1P_1$ chemotypes (**5**, **6**).

The cyclopenta[*b*]indole ring system (**8**) was prepared via a palladium mediated cyclization utilizing aniline **7** and ethyl 2-(2-oxocyclopentyl)acetate as coupling partners (Scheme 1). Subsequent hydroxy-amidine formation (**9**), and treatment with an activated benzoic acid afforded the 5-phenyl-1,2,4-oxadiazole motif (**10**). Ester saponification was typically performed using LiOH, however, compound **17** (Table 1) required a milder procedure

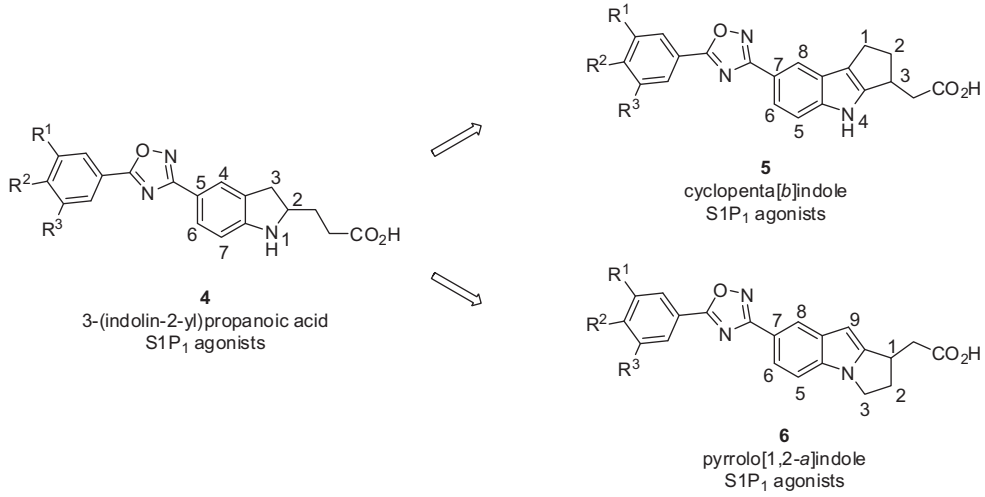

Figure 2. Cyclopenta[*b*]indole and Pyrrolo[1,2-*a*]indole $S1P_1$ agonists.

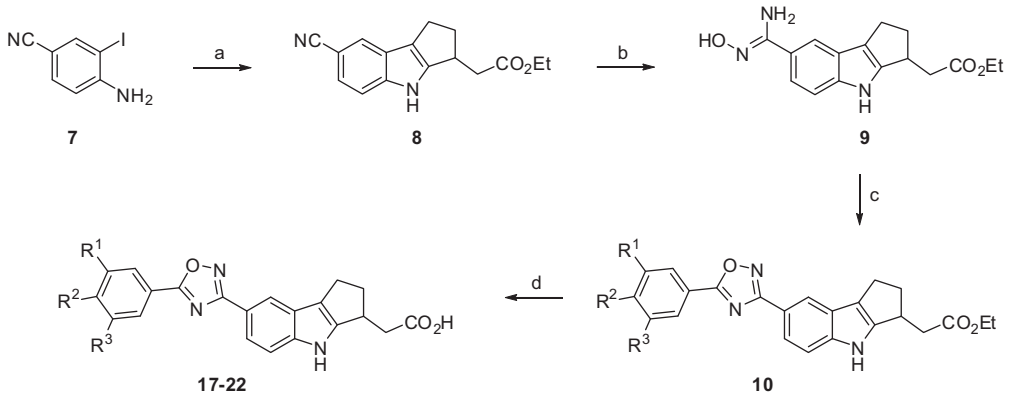

Scheme 1. Cyclopenta[*b*]indole synthesis. (a) Ethyl 2-(2-oxocyclopentyl)acetate, PPTS, $Si(OEt)_4$ then $Pd(OAc)_2$, DIEA (b) 50% aq hydroxylamine, EtOH (c) ArCOCl, Et_3N or $ArCO_2H$, CDI (d) NaOH or LiBr, Et_3N, MeCN, water.

Table 1
Cyclopenta[*b*]indole and Pyrrolo[1,2-*a*]indole SAR

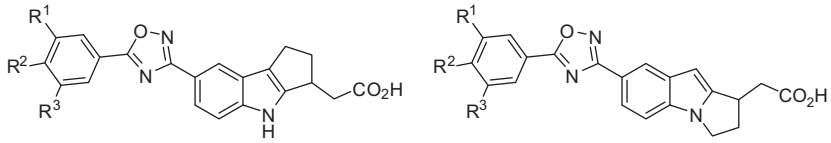

R^1	R^2	R^3	Cmpd	$hS1P_1$ EC_{50}[a] (nM)	Cmpd	$hS1P_1$ EC_{50}[a] (nM)
OCF_3	H	CN	**17**	1.1	**23**	0.25
OCH_3	H	CN	**18**	157	**24**	4.6
CF_3	H	CF_3	**19**	76	**25**	2.1
H	OCF_3	CN	**20**	3.2	**26**	0.59
H	OCH_3	CN	**21**	4.6	**27**	2.9
H	O-*i*Pr	CN	**22**	7.5	**28**	0.61

[a] EC_{50} values were determined in a human cAMP HTRF assay and are the mean of three or more replicates. All compounds afforded a full response relative to S1P in the assay.

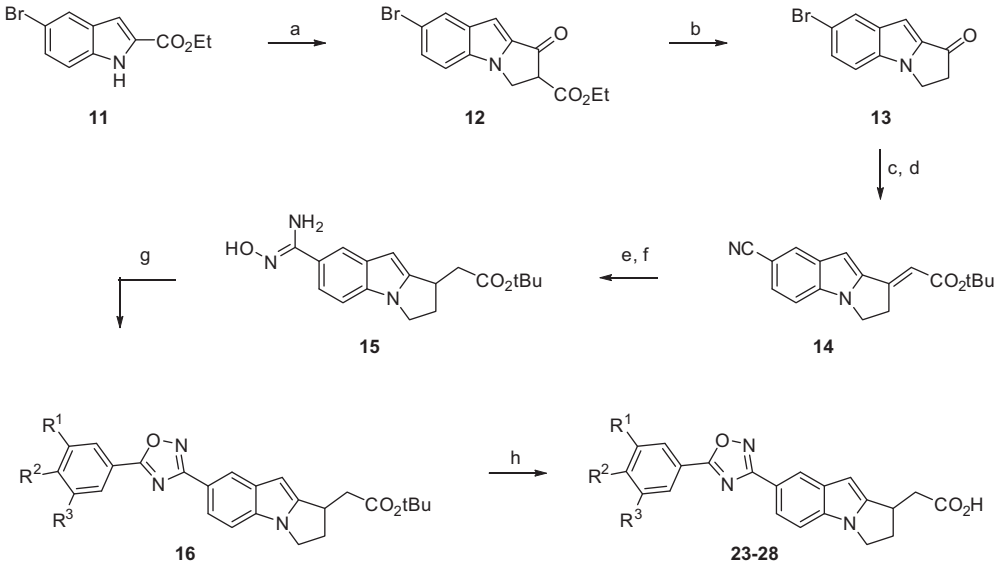

Scheme 2. Pyrrolo[1,2-*a*]indole synthesis. (a) Butyl acrylate, NaH (b) HCl, AcOH (c) $BrPh_3PCHCO_2tBu$, THF (d) CuCN, NMP (e) H_2, Pd/C (f) 50% aq hydroxylamine, EtOH (g) ArCOCl, Et_3N or $ArCO_2H$, CDI (h) TFA, thioanisole/cysteine.

employing lithium bromide in order to avoid reaction at the cyano group.[14]

The pyrrolo[1,2-*a*]indole (**12**) was prepared upon treatment of **11** with butyl acrylate under basic conditions (Scheme 2). Hydrolysis and decarboxylation of the butyl ester gave ketone **13**, which was subjected to a Wittig reaction and subsequent cyanation. Hydrogenation, followed by treatment with hydroxylamine, afforded intermediate **15**, which was used in the oxadiazole forming step (**16**). The *tert*-butyl ester was removed upon treatment with TFA and a cation scavenger.

Human $S1P_1$ potency for several racemic analogs (**17**–**28**) was determined in a HTRF cAMP assay (Table 1). Several structural permutations were examined, of which the 3-cyano-5-trifluoromethoxy-phenyl array appeared to confer the greatest potency across both chemical series. Compounds **17** and **23** were successfully separated into their respective enantiomers by chiral chromatography using a ChiralCelOD® column (**17**, IPA/hexanes) and a ChiralPakADH® column (**23**, MeCN). Stereochemical assignments were not made at this time, but the individual enantiomers were referred to by their elution order (e.g., **17a** first eluting, **17b** second eluting; **23a** first eluting, **23b** second eluting). The resolved enantiomers were subsequently characterized across several pre-clinical species as well as the other human subtypes (Table 2). All four enantiomers maintained a good level of activity for the rodent receptors, and were selective against the human $S1P_2$, $S1P_3$, and $S1P_4$ subtypes. In all cases, significant agonism at the $S1P_5$ receptor was observed. Selectivity data was generated using a DiscoveRX β-arrestin platform,[15] wherein a significant shift in human $S1P_1$ potency was observed. The more potent enantiomer in each chemical series (**17b** and **23b**) was subsequently selected for further evaluation.

ADME profiling revealed good stability in mouse, rat, and human liver microsomes, and **17b** and **23b** were determined to have a terminal half-life of approximately 5 h in male Sprague–Dawley rats after oral administration (Table 3). Both compounds had relatively low systemic clearance and volume of distribution, but **23b** was found to have a higher oral bioavailability achieving plasma concentrations of >10X that of **17b**.

Based on the accepted mechanism of action, a reduction in circulating lymphocytes is an essential requirement for the development of new $S1P_1$ agonists. Compounds **17b** and **23b** were evaluated in a mouse lymphocyte lowering time-course experiment at a 6 mg/kg oral dose (Fig. 3). Both compounds produced a maximal reduction in circulating lymphocytes by the 5 h

Table 2
Cross species $S1P_1$ activity and human subtype selectivity data

	$S1P_1$ EC_{50}[a] [cAMP, nM]			hS1P$_{1-5}$ EC_{50}[a] [β-arrestin, nM]				
	Human	Rat	Mouse	$S1P_1$	$S1P_2$	SIP_3	$S1P_4$	SIP_5
17a	1.73	1.4	8.3	55	>100,000	>100,000	239	11
17b	0.75	1.8	2.6	36	>100,000	>100,000	462	15
23a	0.76	3.4	5.5	123	>100,000	>100,000	>100,000	289
23b	0.08	0.1	0.52	4.8	>100,000	>100,000	>100,000	21

[a] EC_{50} values are the mean of three or more replicates.

Table 3
Microsomal stability and rat pharmacokinetics

Cmpd	LM[a] ($T_{1/2}$)	Male Sprague–Dawley rat pharmacokinetics[b]					
		Cl (L/h/kg)	Vss (L/kg)	$T_{1/2}$ (h)	C_{max} (ng/mL)	AUC_{last} (hr*μg/mL)	%F
17b	>60 min (m, r, h)	0.0834	0.734	5.46	1.40	11.0	32.5
23b	>60 min (r, h)	0.0253	0.234	4.68	13.3	124	100

[a] Microsomal half-life.
[b] 2.0 mg/kg IV (100% PEG400), 3.0 mg/kg PO (0.5% methyl cellulose).

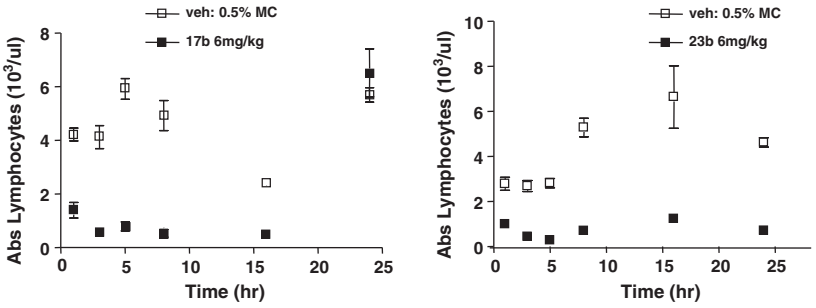

Figure 3. BALB/c mice lymphocyte lowering. Compounds **17b** and **23b** were dosed orally (6 mg/kg) as a suspension in 0.5% methyl cellulose.

time-point, with **23b** maintaining this level of suppression out to 24 h. Lowering the dose of **23b** to 1.0 mg/kg produced an equivalent response at 5 h, but normalization of lymphocyte levels occurred by 24 h.

Both **17b** and **23b** were efficacious in several rodent models of autoimmune disease; however, a much higher dose (30 mg/kg) of **17b** was required to achieve complete suppression of lymphocytes over 24 h and maximal benefit in these chronic studies. Consistent with the 24 h lymphocyte data, **23b** was efficacious at lower doses and showed a clear dose response (Fig. 4 and 5). Compound **23b** was found to be effective in delaying the onset and reducing the severity of disease in a mouse experimental autoimmune encephalomyelitis (EAE) model, a myelin/oligodendrocyte glycoprotein (MOG) 35–55 induced demyelinating autoimmune response similar to MS (Fig. 4).[16] At the highest dose, **23b** showed comparable efficacy to **1** in terms of reduced disease score and incidence. Similarly, this compound was effective at preventing disease in a cyclophosphamide-induced Type I diabetes model performed in non-obese diabetic (NOD) mice (Fig. 5a).[17] Treatment with **23b** maintained normal glucose levels over the duration of the experiment, indicating a reduction in T-cell mediated β-cell destruction and delayed disease progression. Prophylactically, in a collagen induced arthritis (CIA) model performed in female Lewis rats (Fig. 5b),[18] **23b** reduced joint inflammation (as measured by mean ankle diameter) at all doses evaluated. Compound **23b** appeared to exceed the efficacy of the 1 mg/kg dose of (**1**), and approached the

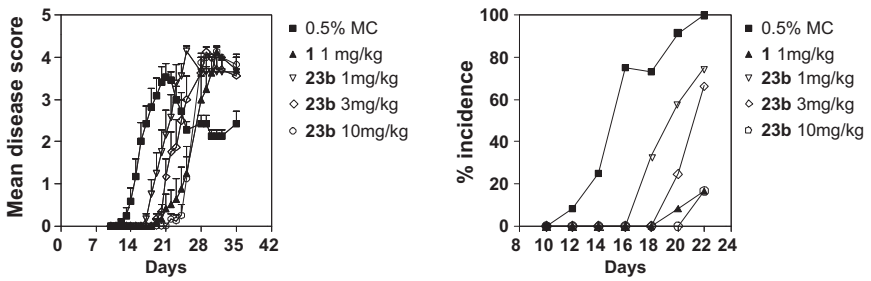

Figure 4. Mouse experimental autoimmune encephalomyelitis (EAE) model. Female C57Bl/6 mice were immunized with MOG35-55 peptide and Freund's complete adjuvant. On day 3 mice were dosed orally (q.d.) with test compound in 0.5% methylcellulose. The animals were monitored daily for signs of disease. Disease severity was graded on a scale of 1–5, with one being limp tail or hind limb weakness and five being death.

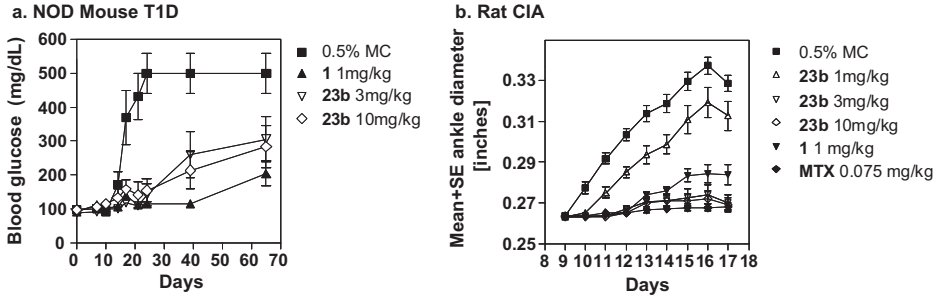

Figure 5. NOD mouse cyclophosphamide-induced Type I diabetes model and rat collagen induced arthritis model. (a) Non–obese diabetic (NOD) mice were dosed with cyclophosphamide (i.p.) on day 0 and 14 to accelerate the onset of diabetes. Oral dosing (q.d.) of test compound in 0.5% methyl cellulose was performed from day 0 to day 25. Animals were considered diabetic if they had a non-fasting blood glucose value >250 mg/dL. (b) Bovine type II collagen emulsified in Freund's complete adjuvant was administered to female Lewis rats on days 0 and 6. Starting on day 0, test compound was delivered orally as a suspension in 0.5% methyl cellulose. Caliper measurements of ankle diameter were taken on days 9–17. MTX = methotrexate.

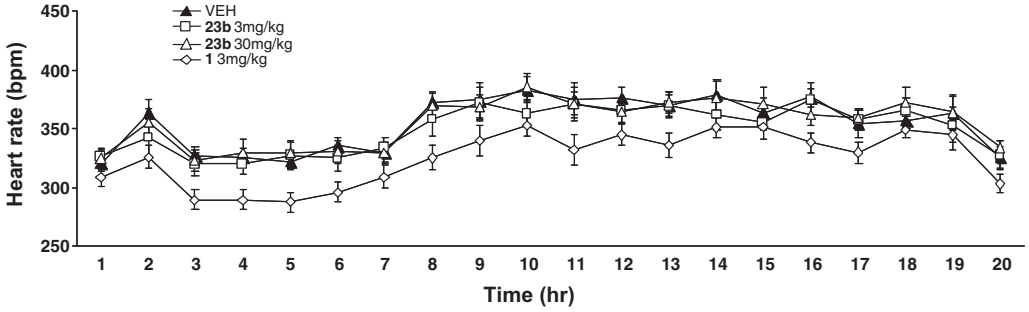

Figure 6. Effects of **23b** on heart rate in telemeterized Charles–River Sprague–Dawley rats. Test compound was dosed orally as a suspension in 0.5% methyl cellulose.

efficacy threshold achieved by methotrexate (MTX) which is a first line therapy for the treatment of rheumatoid arthritis.

In vitro safety profiling included screening for unwanted cross-reactivity at the CYP P450 isozymes and the hERG channel, as well as evaluation of the cytotoxicity and mutagenicity potential. Compound **23b** was not an inhibitor (IC_{50} > 30 μM) of the major CYP P450 isoforms (3A4, 2D6, 2C9, 2C19, 1A2), and no interaction with the hERG channel was observed in astemizole binding (IC_{50} > 30 μM) or in patch clamp (IC_{50} > 400 μM). Little activity was observed in an in vitro cellular toxicity assay measuring changes in membrane integrity (IC_{50} = 25 μM), nuclear size (IC_{50} > 1000 μM), mitochondrial membrane potential (IC_{50} > 1000 μM), and intracellular calcium release (IC_{50} = 346 μM). Ames testing showed no frame shift or base pair mutations in the five strains tested.

Given the bradycardia observed in human trials of **1**, **23b** was examined in telemeterized Sprague–Dawley rats to detect any changes in heart rate. Compound **23b** was dosed orally at 3 and 30 mg/kg and **1** was included as a positive control. Heart rate was measured over a 20 h period and the hourly readings are shown in Figure 6. Consistent with literature reports,[19] **1** produced a pronounced reduction in heart rate in this experiment. Overall, compound **23b** was very similar to the vehicle treated animals, suggesting limited interaction with the rodent $S1P_3$ receptor, and supporting the in vitro findings.

In conclusion, we have identified two new $S1P_1$ chemotypes comprised of a fused tricyclic indole motif. Optimization efforts led to the identification of two lead molecules which possess excellent selectivity against the cardiac expressed $S1P_3$ subtype. In vivo, our most potent compound **23b** demonstrated robust lymphocyte lowering in mouse, which translated into impressive efficacy in three different rodent models of autoimmune disease. Furthermore, this compound was found to have an acceptable in vitro safety profile and did not induce $S1P_3$ mediated bradycardia in rodents. Additional studies for these compounds and other second generation $S1P_1$ agonists will be reported elsewhere in due course.

References and notes

1. (a) Adachi, K.; Kohara, T.; Nakao, N.; Arita, M.; Chiba, K.; Mishina, T.; Sasaki, S.; Fujita, T. *Bioorg. Med. Chem. Lett.* **1995**, *5*, 853; (b) Kiuchi, M.; Adachi, K.; Kohara, T.; Minoguchi, M.; Hanano, T.; Aoki, Y.; Mishina, T.; Arita, M.; Nakao, N.; Ohtsuki, M.; Hoshino, Y.; Teshima, K.; Chiba, K.; Sasaki, S.; Fujita, T. *J. Med. Chem.* **2000**, *43*, 2946.
2. Hale, J.; Yan, L.; Neway, W.; Hajdu, R.; Bergstrom, J.; Milligan, J.; Shei, G.; Chrebet, G.; Thornton, R.; Card, D.; Rosenbach, M.; Rosen, H.; Mandala, S. *Bioorg. Med. Chem. Lett.* **2004**, *12*, 4803.
3. Oo, M.; Thangada, S.; Wu, M.; Liu, C.; Macdonald, T.; Lynch, K.; Lin, C.; Hla, T. *J. Biol. Chem.* **2007**, *282*, 9082.
4. Kappos, L.; Radue, E.; O'Conner, P.; Polman, C.; Hohlfeld, R.; Calabresi, P.; Salmaj, K.; Agoropoulou, C.; Layk, M.; Auberson, L.; Burtin, P. *N. Eng. J. Med.* **2010**, *362*, 387.
5. Choi, J.; Gardell, S.; Herr, D.; Rivera, R.; Lee, C.; Noguchi, K.; Teo, S.; Yung, Y.; Lu, M.; Kennedy, G.; Chun, J. *Proc. Natl. Acad. Sci.* **2011**, *108*, 751.
6. Hamada, M.; Nakamura, M.; Kiuchi, M.; Marukawa, K.; Tomatsu, A.; Shimano, K.; Sato, N.; Sugahara, K.; Asayama, M.; Takagi, K.; Adachi, K. *J. Med. Chem.* **2010**, *53*, 3154.
7. Gergely, P.; Wallström, E.; Nuesslein-Hildesheim, B.; Bruns, C.; Zécri, F.; Cooke, N.; Traebert, M.; Tuntland, T.; Rosenberg, M.; Saltzman, M. *Multiple Sclerosis* **2009**, *15*, S125.
8. http://www.receptos.com/clinical-development-RPC1063.php.
9. Demont, E.; Arpino, S.; Bit, R.; Campbell, C.; Deeks, N.; Desai, S.; Dowell, S.; Gaskin, P.; Gray, J.; Harrison, L.; Haynes, A.; Heightman, T.; Holmes, D.; Humphreys, P.; Kumar, U.; Morse, M.; Osborne, G.; Panshal, T.; Philpott, K.; Taylor, S.; Watson, R.; Willis, R.; Witherington, J. *J. Med. Chem.* **2011**, *54*, 6724.
10. (a) Piali, L.; Froidevaux, S.; Hess, P.; Nayler, O.; Bolli, M.; Schlosser, C.; Steiner, B.; Clozel, M. *J. Pharmacol. Exp. Ther.* **2011**, *337*, 547; (b) Bolli, M.; Abele, S.; Binkert, C.; Bravo, R.; Buchmann, S.; Bur, D.; Gatfield, J.; Hess, P.; Kohl, C.; Mangold, C.; Mathys, B.; Menyhart, K.; Müller, C.; Nayler, O.; Scherz, M.; Schmidt, G.; Sippel, V.; Steiner, B.; Strasser, D.; Treiber, A.; Weller, T. *J. Med. Chem.* **2010**, *53*, 4198; (c) http://www.clinicaltrials.gov/ct2/show/NCT00852670?term=ACT-128800&rank=3.
11. http://clinicaltrials.gov/show/NCT01148810.
12. (a) http://clinicaltrials.gov/show/NCT01375179.; (b) Song, J.; Matsuda, C.; Kai, Y.; Nishida, T.; Nakajima, K.; Mizushima, T.; Kinoshita, M.; Yasue, T.; Sawa, Y.; Ito, T. *J. Pharmacol. Exp. Ther.* **2008**, *324*, 276.

13. Unpublished work.
14. Mattsson, S.; Dahlströrm, M.; Karlsson, S. *Tetrahedron Lett.* **2007**, *48*, 2497.
15. http://www.discoverx.com/gpcrs/arrestin.php.
16. Kataoka, H.; Sugahara, K.; Shimano, K.; Teshima, K.; Koyama, M.; Fukunari, A.; Chiba, K. *Cell. Mol. Immunol.* **2005**, *2*, 439.
17. Brode, S.; Raine, T.; Zaccone, P.; Cooke, A. *J. Immunol.* **2006**, *177*, 6603.
18. (a) Bendele, A. *J. Musculoskelet. Neuron. Interact.* **2001**, *1*, 377; (b) Matsuura, M.; Imayoshi, T.; Okumoto, T. *Int. J. Immunopharmacol.* **2000**, *22*, 323.
19. Forrest, M.; Sun, S.; Hajdu, R.; Bergstrom, J.; Card, D.; Doherty, G.; Hale, J.; Keohane, C.; Meyers, C.; Milligan, J.; Mills, S.; Nomura, N.; Rosen, H.; Rosenbach, M.; Shei, G.; Singer, I.; Tian, M.; West, S.; White, V.; Xie, J.; Proia, R.; Mandala, S. *J. Pharmacol. Exp. Ther.* **2004**, *309*, 758.